Transcriptome alterations in chicken HD11 cells with steady knockdown and overexpression of *RIPK2* gene

Sun Hong-yan,[*,†,1] Li Huan,[‡] Yang Ye-xin,[*] Cao Yu-xuan,[*] Tan Ji-shuang,[*] and Li Na-ying[*]

[*]*College of Animal Science and Technology, Yangzhou University, Yangzhou 225009, China;* [†]*Joint International Research Laboratory of Agriculture & Agri-Product Safety, Ministry of Education, Yangzhou University, Yangzhou 225009, China; and* [‡]*School of Biological and Chemical Engineering, Yangzhou Polytechnic College, Yangzhou 225009, China*

ABSTRACT Receptor interacting protein kinase 2 (**RIPK2**) is involved in a variety of signaling pathway to produce a series of inflammatory cytokines in response to a diverse of bacterial, viral and protozoal pathogens. However, the underlying regulating of *RIPK2* remain unknown. Transcriptome alterations in chicken HD11 cells following *RIPK2* overexpression or silencing by shRNA were analyzed by next-generation sequencing. Both overexpression and knockdown of the *RIPK2* gene caused wide-spread changes in gene expression in chicken HD11 cells. Differentially expressed genes (**DEGs**) caused by altered *RIPK2* gene expression were associated with multiple biological processes linked with biological regulation, response to stimulus, cell communication, and signal transduction etc. KEGG analysis revealed that many of the DEGs were enriched in VEGF signaling pathway, ECM-receptor interaction, Focal adhesion, TGF-beta signaling pathway etc. Moreover, we show that initiation genes, TGFB1 and TGFB3, in the TGF-beta signaling pathway are biological targets regulated by *RIPK2* in chicken HD11 cells. This is the first transcriptome-wide study in which RIPK2-regulated genes in chicken cells have been screened. Our findings elucidate the molecular events associated with *RIPK2* in chicken HD11 cells.

Key words: *RIPK2*, knockdown, overexpression, RNAseq, gene network

2023 Poultry Science 102:102263
https://doi.org/10.1016/j.psj.2022.102263

INTRODUCTION

Receptor interacting protein kinase 2 (**RIPK2**), a member of the RIPK family, is a critical effector of immunity to a diversity of bacterial, viral, and protozoal pathogens as it is an essential adaptor for a variety of signal transduction cascades. Specifically, *RIPK2* could participate in innate and acquired immune responses induced by different pathogens to produce a series of inflammatory cytokines and regulate cell apoptosis (Bist et al., 2014; Hofmann et al., 2021). Previous studies have shown that *RIPK2* mainly exhibited its function through NOD signaling pathway, which is a key and core gene of NOD signaling pathway and a necessary gene to activate ERK and MAPK pathways (Jing et al., 2014; Li et al., 2019). Activation the complex of NOD2: RIPK2 can cause a series of cascade reactions such as autophagy, antigen presentation, and initiation of a series of signaling pathways (Anand et al., 2011; Wu et al., 2018; Lin et al., 2020; Pan et al., 2021; Zhou et al., 2021).

Moreover, *RIPK2* can also participate in many diseases such as pneumonia, multiple sclerosis, asthma, Crohn's disease (Balamayooran et al., 2011; Shaw et al., 2011; Miller et al., 2020), playing an important role in respiratory system immunity. Shimada et al. (2009) have demonstrated that knockout of *RIPK2* in mice could impair iNOS expression and NO production; delay neutrophil recruitment to the lungs; reduce bacterial clearance; and develop more severe and chronic lung inflammation. Meanwhile, it was found that *RIPK2* played a critical role in the activation of central nervous system-infiltrating dendritic cells, as well as in autoimmune encephalomyelitis (Shaw et al., 2011). Besides, Miller et al. (2020) found that *RIPK2* can promote house dust mite-associated allergic airway inflammation and Th2 and Th17 immunity. Inhibition of *RIPK2* can attenuate airway inflammation and remodel airway (Miller et al., 2020), indicating *RIPK2* might be a potential of pharmacological targeting gene in asthma.

Received June 20, 2022.
Accepted October 13, 2022.

[1]Corresponding author: sunhy@yzu.edu.cn

The aforementioned findings reveal that *RIPK2* plays an important role in the recognition of intracellular bacteria, the alleviation of inflammatory responses in different diseases, and the regulation of host immunity. At present, although the function of *RIPK2* gene and its NOD signaling pathway have been studied in human and mice, there are few studies in chickens. Furthermore, the gene networks regulating *RIPK2* are unclear at present.

In the present study, we performed a large-scale analysis of gene expression alterations in chicken HD11 cells induced by *RIPK2* knockdown and overexpression using transcriptome sequencing. Furthermore, we identified the genes involved in the TGF-beta signaling pathway as targets of *RIPK2* regulation in chicken HD11 cells. These results have provided new insights into the role of *RIPK2* in chicken.

MATERIALS AND METHODS

Ethics Statement and Experimental Animals

The procedures involving animals and their care conformed to the U.S. National Institute of Health guidelines (NIH Pub. No. 85-23, revised 1996). The experiments were conducted under the approval of the Ethics Committee of Yangzhou University for Laboratory and Experimental Animals. The chickens used in this study were obtained from the TIANGE QINYE Co., Ltd. The experimental procedures were approved by the Institutional Animal Care and Use.

Experiment and Data Acquisition

The RNA-seq data of bone marrow were from our previous experiment, which can be downloaded from Gene Expression Omnibus (**GEO**) with accession numbers GSE67302. The detailed information of bone marrow RNA-seq experiment can be found in the study of Sun et al. (2015). Briefly, 4 wk commercial male broilers were challenged with 0.1 mL 1×10^8 cfu APEC O1 via the left intra-air sac injection. The control birds were injected with 0.1 mL PBS with the same route. Bone marrow was collected at 5 days postinfection (**dpi**). The infected birds were categorized into resistant and susceptible based on internal lesion scores according to the study of Peighambari et al. (2000). The lesion score of the resistant birds was 0−1, while that of susceptible birds were 6−7. Then, a total of 3 treatments were generated: control birds, resistant birds, and susceptible birds.

Analysis of RIPK2 Gene Expression Patterns

A total of 13 tissues (heart, cecum, stomach, liver, small intestine, duodenum, lung, harderian glands, bone marrow, bursa, thymus, spleen, and blood) were collected respectively from four 4 wk of age commercial male broilers. Total RNA was extracted with Trizol reagent (Invitrogen, Carlsbad, CA) to identify the *RIPK2* gene expression pattern by using RT-qPCR.

Cell Culture

The chicken HD11 cell line was kindly provided by Dr. Xuming Hu (Yangzhou University). The chicken macrophage-like cell line HD11 was maintained in RPMI1640 (Gibco, Carlsbad, CA) supplemented with 10% fetal bovine serum (**FBS**, Gibco) in a humidified incubator with 5% CO_2 at 37°C, and cells were passaged before 80 to 90% confluence.

Cell Transfection and Infection

Small hairpin *RIPK2* (**shRIPK2**) plasmid (Table S1) and pcDNA3.1-RIPK2 (oeRIPK2) were synthesized by GenePharma (Shanghai, China). The recombinant vector (shRIPK2 with high interference efficiency and oeRIPK2) were packaged with lentivirus. The lentivirus titer is 2×10^8 TU/mL. 1×10^5 cells /well were seeded in the 24 well plate. The cells were then infected with lentivirus with MOI = 40 by using the lipofectamine 2000 reagent (Invitrogen, Carlsbad, CA). After 48 h of cell culture in 37℃ with 5% CO_2 for shRIPK2 and oeRIPK2 group, 10 μg/mL purinomycin medium was added in the cells. Then, the positive clones were screened for four generations, and finally the HD11 cells with steady overexpression/knockdown of *RIPK2* gene was obtained. For induction with LPS, HD11 cells with steady knockdown or overexpression of *RIPK2* were challenged with 1 μg/mL LPS for 24 h.

Apoptosis Assay

Cell apoptosis was evaluated using an annexin V-PE/7-AAD apoptosis detection Kit (Vazyme, Nanjing, China). In brief, cells (5×10^5 cells/well) were divided into different groups and seeded in 6-well plates. After transfection, the cells were placed in 500 μL of a binding buffer (Biosea Biotechnology, Beijing, China), treated using 5 μL of annexin V-PE and 10 μL of 7-AAD, maintained for 30 min at 25°C in the dark. Stained cells were detected and analyzed using flow cytometry (Becton Dickinson, Franklin Lakes, NJ). Each experiment was performed in triplicate.

Transcriptome Sequencing and Gene Expression Quantitation

Total RNA was extracted from HD11 cells of wild type group (**WT**), knockdown of *RIPK2* group (shRIPK2), and overexpression of *RIPK2* group (oeRIPK2) using an RNA isolation kit (QIAGEN, Hilden, Germany) according to the manufacturer's protocol. The quality of RNA was analyzed by agarose gel electrophoresis and a Nanodrop OneCspectrophotometer (Thermo Fisher Scientifc Inc., MA). The RNA Integrity was confirmed by Qseq (Qseq100, Guangding, Taiwan). A total of 2 μg of RNA

was used for stranded RNA sequencing library preparation using Ribo-of rRNA depletion kit (Catalog NO. MRZG12324, Illumina, San Diego, CA) following the manufacturer's instruction. The library products corresponding to 200 to 500 bps were enriched, quantified, and finally sequenced on NovaSeq 6000 sequencer (Illumina) with PE150 sequencing platform.

For quality control, raw data were filtered by Trimmomatic (version 0.36). The obtained clean reads were further treated with in-house scripts to eliminate duplication bias introduced in library preparation and sequencing. Deduplicated reads were mapped to the reference genome of the chicken (*Gallus gallus*) from Ensembl (https://asia.ensembl.org/info/data/ftp/index.html) using STRA software (version 2.5.3a) with default parameters. Reads mapped to the exon regions of each gene were counted by featureCounts (Subread-1.5.1; Bioconductor) and then RPKM was calculated. Differentially expressed genes (**DEGs**) between groups were identified using the edgeR package (version 3.12.1). A *P*-value cutoff of 0.05 and fold-change cutoff of 1.5 were used to judge the statistical significance of gene expression differences.

Functional Categorization

GO analysis (Huang et al., 2009a) and KEGG enrichment analysis (Kanehisa and Goto, 2000; Huang et al., 2009b) for DEGs were both implemented by KOBAS software (version: 2.1.1) with a *P*-value cutoff of 0.05 to judge statistically significant enrichment.

Quantitative Real-Time PCR Assay

The RNA from different experiments was reverse transcribed into cDNA using a Reverse Transcription Kit (Takara, Dalian, China). The One Step SYBR PrimeScript PLUS RTRNA PCR Kit (Takara, Dalian, China) was used for cDNA synthesis. RT-qPCR was conducted using a SYBR Premix Ex Taq II kit (Takara) to evaluate the expression level of *GAPDH, RIPK2, HSPB1, JUN, FOS, CASP3, BCL2L11, CD44, CD36, TNFSF8, PDK4, IRF1, PAK3*, and *CXCR1*. Primer sequences are displayed in Table S2. RT-qPCR thermal cycling conditions were as follows: denaturation for 3 min at 95°C, 40 cycles of 10 s at 95°C, 58°C for 30 s, and then 72°C for 30 s. Relative expression of above genes were calculated using the $2^{-\Delta\Delta Ct}$ method and *GAPDH* was utilized as an internal control. The formula of ΔΔCt is (Ct of gene in test group - Ct of *GAPDH* in test group) - (Ct of gene in control group − Ct of *GAPDH* in control group).

Western Blotting

Cells from each of the 3 groups were lysed on ice using 200 μL RIPA bufer (Beyotime Biotechnology, Shanghai, China) for 30 min. Next, the lysis mixtures were centrifuged and the supernatants were collected. BCA Protein Assay Kit (Pierce, Appleton, WI,) was used for quantification of proteins. Then, the isolated proteins were subjected to sodium dodecyl sulfate-polyacrylamide gel (**SDS-PAGE**) and electrophoretically transferred to PVDF membranes. Afterwards, membranes were blocked in 5% BSA for 2 h at room temperature and then probed with the primary antibodies at 4°C overnight. The primary antibodies included anti-GAPDH (ab181602, Abcam, Cambridge, MA), anti-RIPK2 (70R-10,459, Fitzgerald, North Acton, MA), anti-TGFB1 (ab9758, Abcam), and anti-TGFB3 (ab15537, Abcam) were used at a dilution of 1:1,000. Then the membranes were incubated with secondary antibodies tagged with horseradish peroxidas (Sigma-Aldrich, St. Louis, MI) at a 1:10,000 dilution at room temperature for 2 h. Then, immunoblots were visualized by enhanced chemiluminescence (ECL kit, Santa Cruz Biotechnology, Dallas, TX). The blots were visualized by using Image Lab Software (Bio-Rad, Hercules, CA).

Statistical Analysis

All data were presented as mean ± standard error. Statistical analysis was performed using JMP statistical software (version 15.2.1, SAS Institute). Differential gene expression was analyzed using Student's *t* test for 2 groups and one-way ANOVA with Tukey Honestly Significant differences test (HSD; SAS, 2000; Cary, NC). $P < 0.05$ was considered significant.

RESULTS

Screening of RIPK2, a Key Candidate Gene for Host Against Bacteria Infection

Bone marrow was collected from wild type birds (Non-infected APEC birds), susceptible birds (APEC-infected birds), and resistant birds (APEC-infected birds), and then performed by RNAseq (Sun et al., 2015). According to the results, 2,804, 1,873, and 2 differentially expressed genes (DEGs) were found in the comparison of Susceptible vs. Wild type birds, Susceptible vs. Resistant birds, and Resistant vs. Wild type birds, respectively. Then, transcriptome sequencing data were analyzed by Venn between Susceptible vs. Resistant birds and Susceptible vs. Wild type birds to find key candidate genes and pathways against APEC infection. A total of 1731 DEGs were identified and involved in 33 significantly changed pathways, of which NOD/RIPK2 signaling pathway had the smallest corrected *P* value (Figure 1A). The expression of DEGs involved in NOD/RIPK2 signaling pathway was displayed in Figure 1B. Since *RIPK2* was the core and key gene in NOD/RIPK2 signaling pathway and had a high expression level in the comparison of Susceptible vs. Resistant birds at 5 d post APEC infection, we speculate that it may play a critical role in host against bacterial infection.

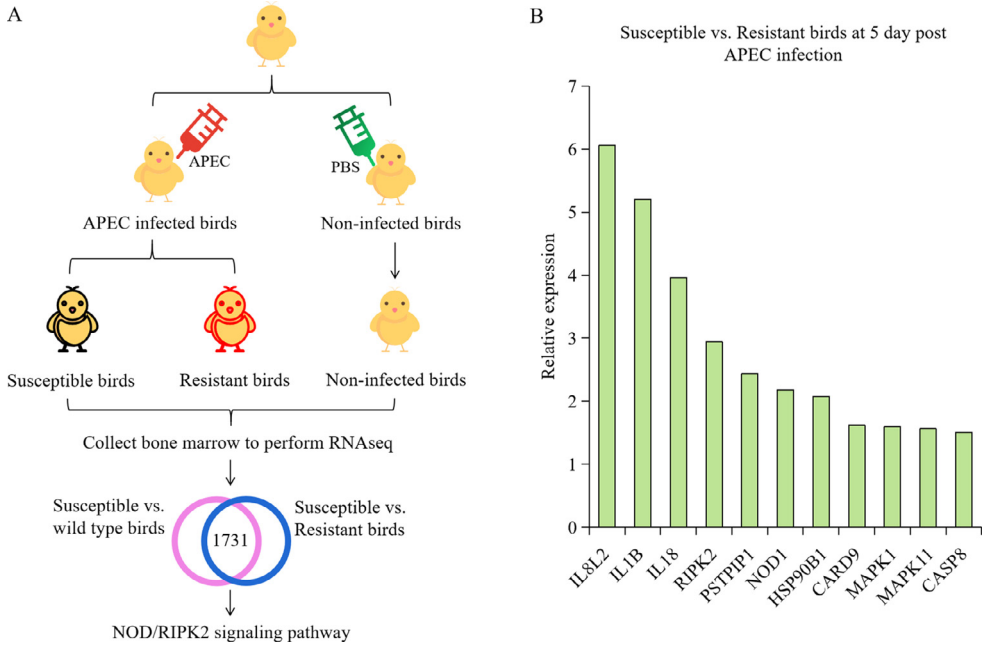

Figure 1. Screening of *RIPK2* from different phenotype chicken by using RNAseq. (A) Experimental design of RNAseq analysis. (B) The relative expression level of the differentially expressed genes involved in NOD/RIPK2 signaling pathway in the comparison of Susceptible vs. Resistant birds at 5 days post APEC infection.

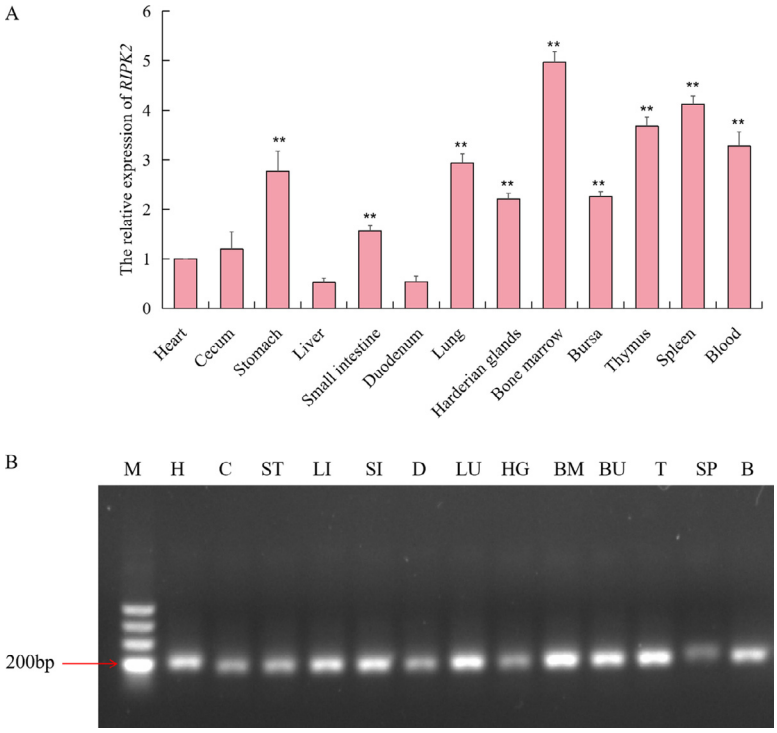

Figure 2. Relative expression pattern of chicken *RIPK2* gene in different tissues. (A) The relative mRNA expression level of *RIPK2* in cecum, stomach, liver, small intestine, duodenum, lung, harderian glands, bone marrow, bursa, thymus, spleen, and blood were measured by using RT-qPCR. The result was normalized with *GAPDH* gene and relative to gene expression in the heart group. ** indicates $P < 0.01$. (B) The agarose gel electrophoresis results of RT-qPCR amplification products. Abbreviations: B, blood; BM, bone marrow; BU, bursa; C, cecum; D, duodenum; H, heart; HG, harderian gland; LI, liver; LU, lung; M, marker; SI, small intestine; SP, spleen; ST, stomach; T, thymus.

Expression Level of RIPK2 *in Different Tissues*

Total RNA was extracted from 13 tissues (heart, cecum, stomach, liver, small intestine, duodenum, lung, harderian glands, bone marrow, bursa, thymus, spleen, and blood). RT-qPCR was used to analyze the mRNA expression levels of *RIPK2* in different tissues. Compared with the heart, the relative *RIPK2* expression level in other tissues was measured as shown in Figure 2. The mRNA expression level of *RIPK2* gene was highest in the bone marrow ($P < 0.01$) compared to other tissues, followed by spleen, blood, thymus, bursa, lung, stomach, harderian glands, small intestine, and cecum. However, the liver tissue had the smallest mRNA expression level of

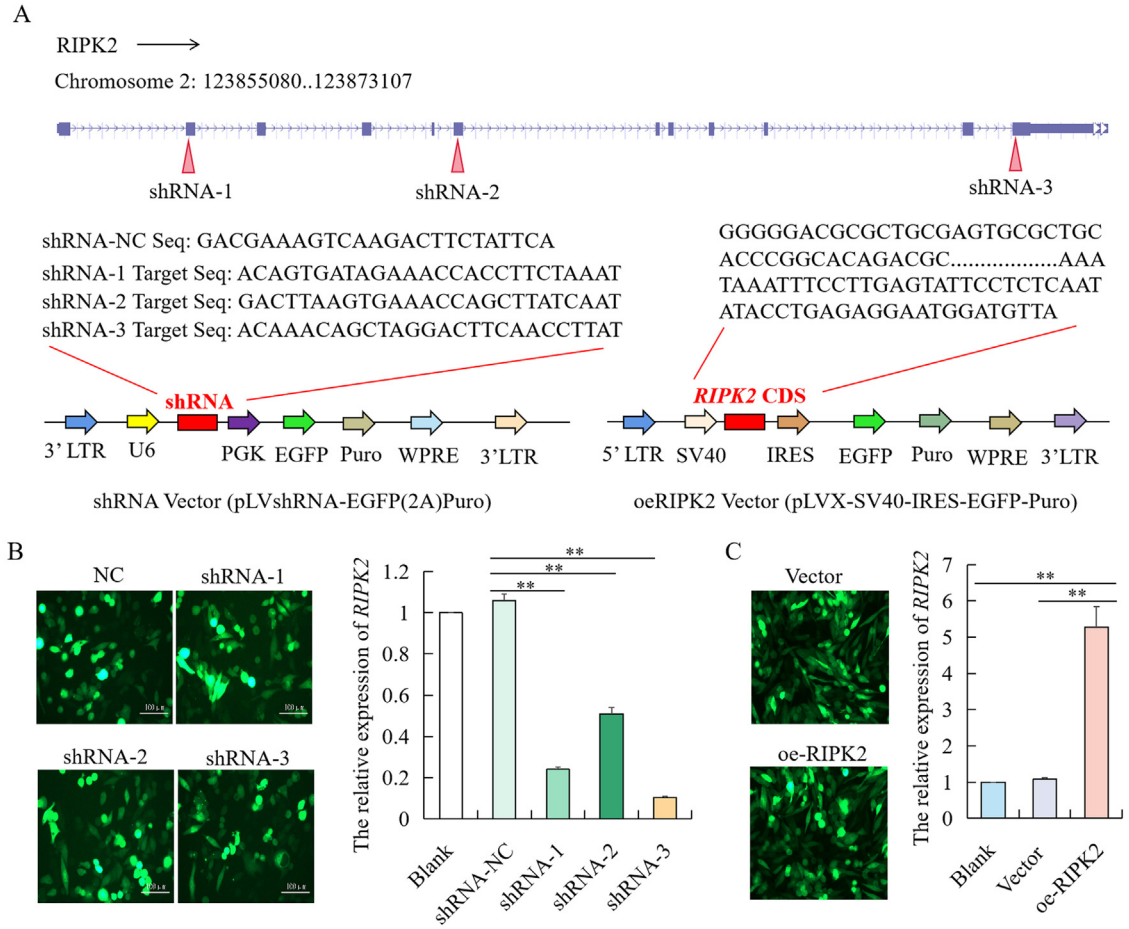

Figure 3. Construction and activity verification of *RIPK2* RNA interference/overexpression vector. (A) RNA interference and overexpression vector design of *RIPK2*. (B) The GFP fluorescence was detected in HD11 cells in vitro indicating effective lentivirus infection. Relative expression of *RIPK2* in HD11 cells transfected with lentiviral shRNA vectors for 48 h as measured by RT-qPCR. shRNA-3 vector has best effect on interfering the expression of *RIPK2*. Scale bars = 100 μm. (C) The GFP fluorescence was detected in HD11 cells in vitro indicating effective lentivirus infection. Relative expression of *RIPK2* in HD11 cells transfected with lentiviral overexpression vector for 48 h as measured by RT-qPCR. Scale bars = 100 μm. ** $P < 0.01$. All values are mean±SD. n = 4.

RIPK2 gene compared with heart tissues, followed by duodenum.

Construction of Overexpression and Interference Lentiviral Vector of RIPK2

To determine the target genes of *RIPK2*, the lentivirus interference and overexpression vector of *RIPK2* were designed and constructed (Figure 3A). The constructed vector with GFP fluorescent protein labeling was transfected into chicken HD11 cells. A large number of fluorescent expressions was observed after 48 h transfection with the constructed vector (Figures 3B and 3C), indicating the vectors can be successfully transfected and effectively expressed in vitro. Moreover, after interfering with *RIPK2*, the interference vector 1, 2, and 3 could significantly reduce the mRNA expression level of *RIPK2* gene ($P < 0.01$), of which interference vector 3 can strongest affect the *RIPK2* expression and was selected to package lentivirus for follow-up experiments (Figure 3B). Meanwhile, the overexpression vector can significantly increase the mRNA expression level of *RIPK2* gene (Figure 3C). In summary, the recombinant vector could effectively interfere/overexpress *RIPK2* in chicken HD11 cells in vitro.

Expression Level of RIPK2 *in HD11 Cells With Steady Knockdown and Oveexpression of* RIPK2

After 48 h transfection with 20 μL of lentivirus encapsulated shRIPK2-3 vector, chicken HD11 cells were cultured with 10 μg/mL puromycin and incubated four generation to obtain the steady *RIPK2* knockdown HD11 cells. The steady *RIPK2* overexpression HD11 cells were also obtained with the same method. To identify the activity of *RIPK2*, the protein and mRNA levels were measured in wild type HD11 cells (WT), HD11 cells with knockdown of *RIPK2* (shRIPK2), and HD11 cells with overexpression of *RIPK2* (oeRIPK2). As shown in Figure 4A and B, a significantly decreased mRNA and protein expression level of RIPK2 were observed in the *RIPK2* knockdown group in comparison to WT ($P < 0.05$), indicating the expression of *RIPK2* was indeed inhibited. Also, the oeRIPK2 group can significantly increase mRNA and protein abundance of

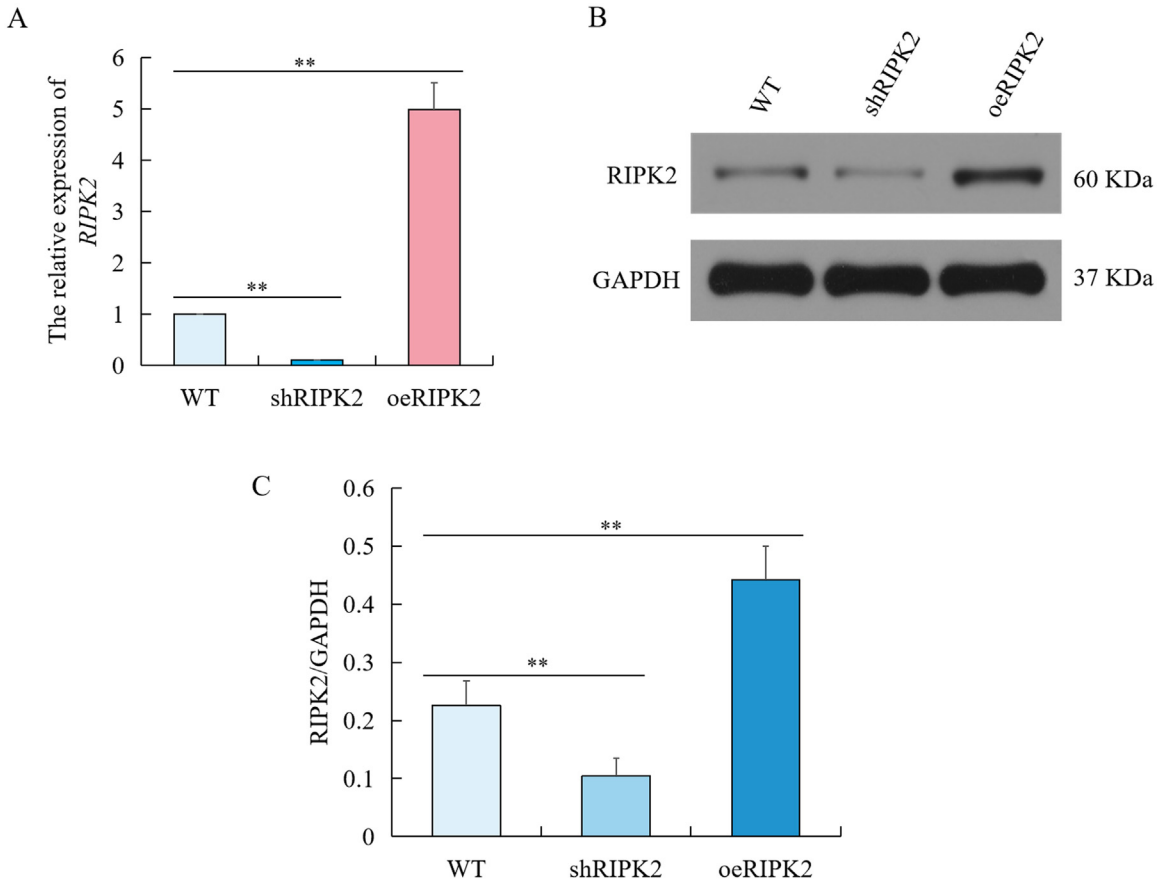

Figure 4. The RIPK2 expression level in chicken HD11 cells with knockdown or overexpression of *RIPK2*. (A) The relative *RIPK2* mRNA expression level in wild type HD11 cells (WT), knockdown of *RIPK2* HD11 cells (shRIPK2), and overexpression of *RIPK2* HD11 cells (oeRIPK2). (B) The RIPK2 protein expression level in wild type HD11 cells (WT), knockdown of *RIPK2* HD11 cells (shRIPK2), and overexpression of *RIPK2* HD11 cells (oeRIPK2) was analyzed by western blot. (C) Image J software was used for RIPK2 gray-level analysis of western blot results. ** $P < 0.01$. All values are mean±SD. n = 4.

RIPK2 compared with WT ($P < 0.05$). In summary, we had successfully constructed the steady *RIPK2* knockdown and overexpression HD11 cells.

Knockdown of RIPK2 *Alleviate Cell Injuries and Overexpression of* RIPK2 *Enhanced Cell Injuries in LPS-Induced Cells*

To identify the function of *RIPK2* during bacterial infection, the effects of *RIPK2* on LPS-induced injuries in chicken HD11 cells were analyzed. Overexpression of *RIPK2* can aggravate LPS-induced injuries in cells by decreasing viability (Figures 5A and 5B), increasing apoptosis (Figures 5A and 5C). However, inhibition of *RIPK2* exhibited the contrary effects on chicken HD11 cells. The viability was improved (Figures 5A and 5B), and apoptosis was inhibited (Figures 5A and 5C). These data suggested that knockdown of *RIPK2* can alleviate inflammatory injuries in chicken HD11 cells.

RNA-Seq and Data Analysis

A total of nine cDNA libraries were constructed, respectively, from WT (n = 3), shRIPK2 (n = 3), and oeRIPK2 (n = 3). The quality control of sequencing data is shown in Table 1. In general, an average of 79,839,400 (range from 71,438,338 to 89,995,934) raw reads was obtained (Table 1). After removing adaptors and low quality reads, each sample yielded approximately 77,545,511 clean reads (range from 69,393,540 to 87,645,300, Table 1). Moreover, unique identifier (**UID**) was also used to remove the duplication data, resulting in a total of 48,275,868 to 60,443,170 UID reads (Table 1). The average of GC content of clean reads was 54.27% (Table 1).

Moreover, 92.81 to 94.83% of the UID reads were found to successfully map to the chicken reference genome (*Gallus gallus* 6.0), of which 86.14 to 91.25% were uniquely mapped to genome (Table 2). Additionally, Table 3 shows the information on the fraction of reads mapping to features for each sample, that is, any expressed parts of the genome. Interestingly, oeRIPK2 group had the largest percentage of reads mapping to coding sequence (CDS, average percentage = 63.98%), followed by shRIPK2 (average percentage = 59.91%), and WT group (average percentage = 59.78%). However, oeRIPK2 group had the smallest percentage of reads mapping to intron (average percentage = 17.84%) compared to shRIPK2 (average percentage = 19.19%) and WT group (average percentage = 19.41%).

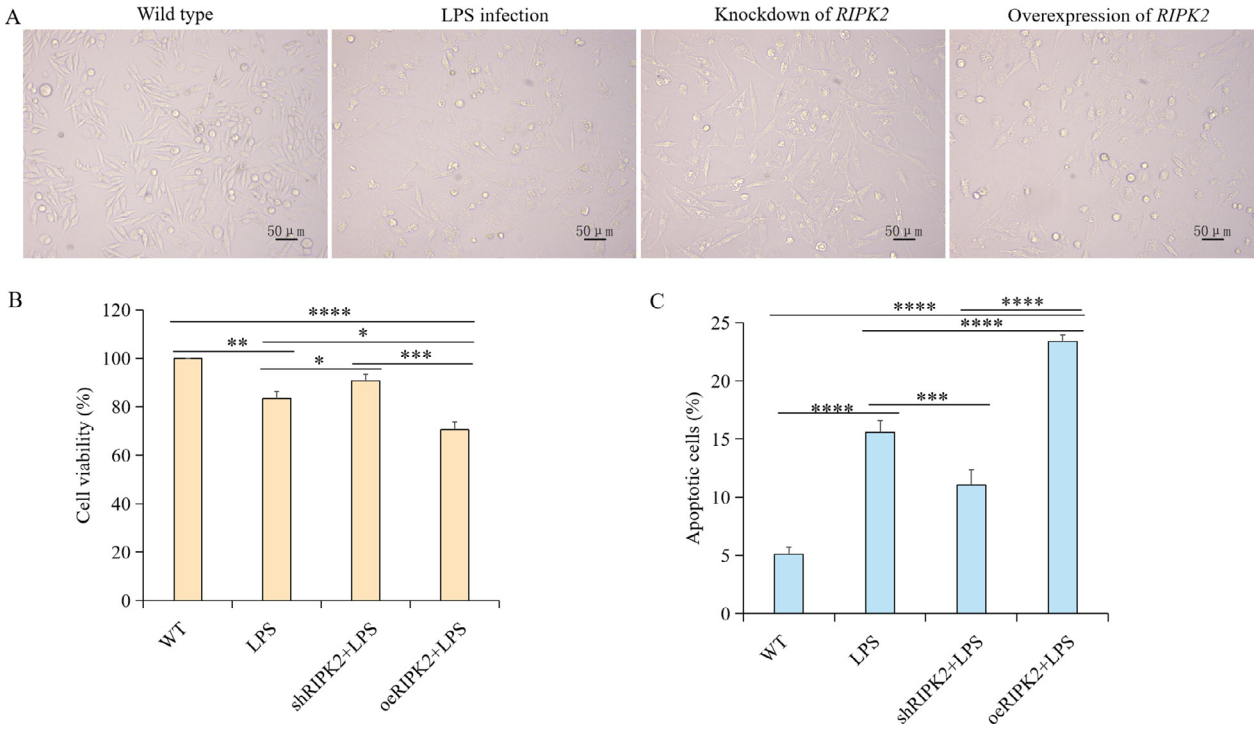

Figure 5. Overexpression of *RIPK2* enhanced cell injuries and inhibition of *RIPK2* attenuated cell injuries in LPS-injured HD11 cells. (A) The morphology of chicken HD11 macrophages in the group of wild type HD11 cells, LPS infected HD11 cells, knockdown of *RIPK2* HD11 cells combine with LPS infection, and overexpression of *RIPK2* HD11 cells combined with LPS infection. (B and C) Cell viability (B) and apoptotic cell rates (C) were respectively measured by CCK8 assay and flow cytometry. * $P < 0.05$; ** $P < 0.01$; *** $P < 0.001$; **** $P < 0.0001$. All values are mean±SD. n = 4.

Table 1. Characteristics of RNA sequencing data before or after quality control.

Sample	Raw bases (G)	Raw reads	Clean reads	Barcoded reads	UID reads	Clean GC (%)	UID GC (%)
WT_1	11.98	79,898,294	77,586,290	74,670,816	55,232,248	51.52	51.23
WT_2	11.71	78,068,340	75,776,170	72,942,218	54,688,864	52.42	52.18
WT_3	11.7	77,977,654	75,414,976	72,679,902	55,110,018	52.74	52.48
shRIPK2_1	13.5	89,995,934	87,645,300	84,359,058	60,443,170	52.29	52.03
shRIPK2_2	12.21	81,387,452	79,241,946	76,218,648	55,397,950	52.79	52.56
shRIPK2_3	10.72	71,438,338	69,393,540	66,598,758	49,039,816	52.87	52.68
oeRIPK2_1	12.64	84,298,680	81,939,736	78,728,740	52,523,330	57.75	58.04
oeRIPK2_2	11.99	79,934,038	77,600,014	74,471,476	49,700,234	57.92	58.23
oeRIPK2_3	11.33	75,555,872	73,311,626	70,331,404	48,275,868	58.17	58.47

Table 2. The reads mapping information for each sample.

Sample	Total reads	Total mapped (%)	Non-unique (%)	Unique (%)	Unmapped reads (%)
WT_1	55,232,248	51,589,617 (93.40)	4,512,427 (8.75)	47,077,190 (91.25)	3,642,631 (6.60)
WT_2	54,688,864	50,974,341 (93.21)	5,295,239 (10.39)	45,679,102 (89.61)	3,714,523 (6.79)
WT_3	55,110,018	51,275,004 (93.04)	5,560,473 (10.84)	45,714,531 (89.16)	3,835,014 (6.96)
shRIPK2_1	60,443,170	56,229,954 (93.03)	5,568,658 (9.90)	50,661,296 (90.10)	4,213,216 (6.97)
shRIPK2_2	55,397,950	51,447,994 (92.87)	5,360,132 (10.42)	46,087,862 (89.58)	3,949,956 (7.13)
shRIPK2_3	49,039,816	45,515,322 (92.81)	4,758,486 (10.45)	40,756,836 (89.55)	3,524,494 (7.19)
oeRIPK2_1	52,523,330	49,808,150 (94.83)	6,498,577 (13.05)	43,309,573 (86.95)	2,715,180 (5.17)
oeRIPK2_2	49,700,234	47,092,760 (94.75)	6,267,916 (13.31)	40,824,844 (86.69)	2,607,474 (5.25)
oeRIPK2_3	48,275,868	45,668,372 (94.60)	6,331,033 (13.86)	39,337,339 (86.14)	2,607,496 (5.40)

Differentially Expressed Genes in HD11 Cells With Altered RIPK2 *Expression Analyzed by Transcriptome Sequencing*

To explore the gene network regulated by chicken *RIPK2*, we performed transcriptome sequencing using chicken HD11 cells with overexpression of *RIPK2* gene (oeRIPK2) or with silenced *RIPK2* gene expression using shRNA (shRIPK2), and wild type HD11 cells (WT). As shown in Figure 6A, the gene expression pattern of WT group was more similar with that in shRIPK2 group, whereas the expression pattern of oeRIPK2 group was

Table 3. The distribution of reads in chicken genome.

Sample	TSS 10 kb (%)	TSS 5 kb (%)	TSS 1 kb (%)	5′ UTR (%)	CDS (%)	3′ UTR (%)	TES 1 kb (%)	TES 5 kb (%)	TES 10 kb (%)	Intergenic (%)	Intron (%)
WT_1	817,934 (1.09)	465,652 (0.62)	264,356 (0.35)	1,709,799 (2.29)	44,927,089 (60.14)	3,539,667 (4.74)	894,691 (1.20)	1,329,951 (1.78)	951,088 (1.27)	5,371,654 (7.19)	14,436,393 (19.32)
WT_2	850,628 (1.16)	481,034 (0.65)	266,795 (0.36)	1,783,041 (2.43)	43,890,294 (59.73)	3,326,499 (4.53)	809,810 (1.10)	1,233,127 (1.68)	961,875 (1.31)	5,646,153 (7.68)	14,229,717 (19.37)
WT_3	854,892 (1.16)	484,649 (0.66)	270,098 (0.37)	1,807,517 (2.45)	43,846,172 (59.48)	3,296,988 (4.47)	796,623 (1.08)	1,220,494 (1.66)	969,557 (1.32)	5,770,236 (7.83)	14,400,640 (19.53)
shRIPK2_1	901,795 (1.11)	542,484 (0.67)	298,909 (0.37)	1,883,579 (2.31)	48,547,638 (59.62)	4,049,765 (4.97)	913,946 (1.12)	1,340,140 (1.65)	975,162 (1.20)	6,235,343 (7.66)	15,737,712 (19.33)
shRIPK2_2	811,832 (1.09)	499,462 (0.67)	276,288 (0.37)	1,758,489 (2.36)	44,794,360 (60.05)	3,562,251 (4.78)	799,364 (1.07)	1,188,481 (1.59)	903,916 (1.21)	5,775,924 (7.74)	14,220,256 (19.06)
shRIPK2_3	712,708 (1.08)	435,538 (0.66)	246,408 (0.37)	1,554,302 (2.36)	39,621,169 (60.05)	3,136,809 (4.75)	702,608 (1.06)	1,046,395 (1.59)	807,534 (1.22)	5,049,179 (7.65)	12,662,782 (19.19)
oeRIPK2_1	441,249 (0.58)	394,763 (0.52)	329,983 (0.44)	2,477,055 (3.27)	48,553,294 (64.18)	3,775,378 (4.99)	651,556 (0.86)	660,678 (0.87)	129,557 (0.17)	4,916,168 (6.50)	13,317,781 (17.61)
oeRIPK2_2	411,770 (0.58)	376,256 (0.53)	312,802 (0.44)	2,339,346 (3.27)	45,823,392 (64.13)	3,504,274 (4.90)	602,633 (0.84)	616,911 (0.86)	125,823 (0.18)	4,691,385 (6.57)	12,647,311 (17.70)
oeRIPK2_3	402,649 (0.58)	365,632 (0.53)	302,814 (0.44)	2,260,234 (3.28)	43,903,993 (63.62)	3,316,619 (4.81)	575,056 (0.83)	588,333 (0.85)	123,578 (0.18)	4,611,458 (6.68)	12,558,893 (18.20)

completely different from WT and shRIPK2 group. Compared with WT group, 1,472 and 1,133 DEGs were identified to be upregulated and downregulated, respectively, in shRIPK2 group (Figure 6B), while 5,053 and 5,416 genes was significantly high expressed and low expressed, respectively, in oeRIPK2 group (Figure 6C). It was found that 4,881 and 5,416 were significantly upregulated and down-regulated, respectively, in the comparison of oeRIPK2 vs. shRIPK2 (Figure 6D). The distribution of $\log_2$(fold change) in shRIPK2 vs. WT was ranged from −3.5 to 3.5, whereas those in oeRIPK2 vs. WT and oeRIPK2 vs. shRIPK2 were from −12 to 12 (Figure 6E). Moreover, 1,670 overlapped DEGs were identified in the three comparisons (Figure 6F).

Functional Annotation of DEGs in Different Comparisons

The gene ontology (**GO**) classification system was used to classify the possible functions of DEGs in different comparisons. A total of 734 genes (28.18%), 1,476 (31.46%), and 3,193 (31%) were successfully assigned to at least one GO term annotation in shRIPK2 vs. WT, oeRIPK2 vs. WT, and oeRIPK2 vs. shRIPK2, respectively. The GO enrichment analysis of DEGs in shRIPK2 vs. WT showed that a total of 404 terms were enriched, including regulation of cellular process, regulation of biological process, biological regulation, and binding etc (Figure 7A). A total of 1,010 significant GO terms were identified in the comparison of oeRIPK2 vs. shRIPK2, of which the top 20 GO terms were similar with shRIPK2 vs. WT (Figure 7C). Moreover, 1,042 GO terms were preferentially enriched in cellular process, regulation of biological process, response to stimulus, gene expression etc. (Figure 7B).

Then, Kyoto Encyclopedia of Genes and Genomes (**KEGG**) classification system was also performed to identify the possible functions of DEGs. A total of 15, 85, and 86 significantly changed pathways were identified in shRIPK2 vs. WT (Table S3), oeRIPK2 vs. WT (Table S4), and oeRIPK2 vs. shRIPK2 (Table S5), respectively. Moreover, A total of 11 significantly changed pathways were detected to be overlapped in the 3 comparisons, which mainly included "Herpes simplex infection", "Focal adhesion", "MAPK signaling pathway", "ECM-receptor interaction", "Lysosome", " VEGF signaling pathway", "Phagosome", and "Apoptosis" etc. (Figure 7D). More remarkable, the significantly changed pathway "Notch signaling pathway (cell growth and differentiation, cell fate decisions)", "TGF-beta signaling pathway (cell proliferation, apoptosis, differentiation, and migration)", "Cell cycle (cell division)", and "Oxidative phosphorylation (cellular respiration)" were enriched in both oeRIPK2 vs. WT and oeRIPK2 vs. shRIPK2.

Verification of RNAseq Data by RT-qPCR

To validate the reliability of RNA-seq data, 12 DEGs overlapped in the 3 comparisons were randomly selected

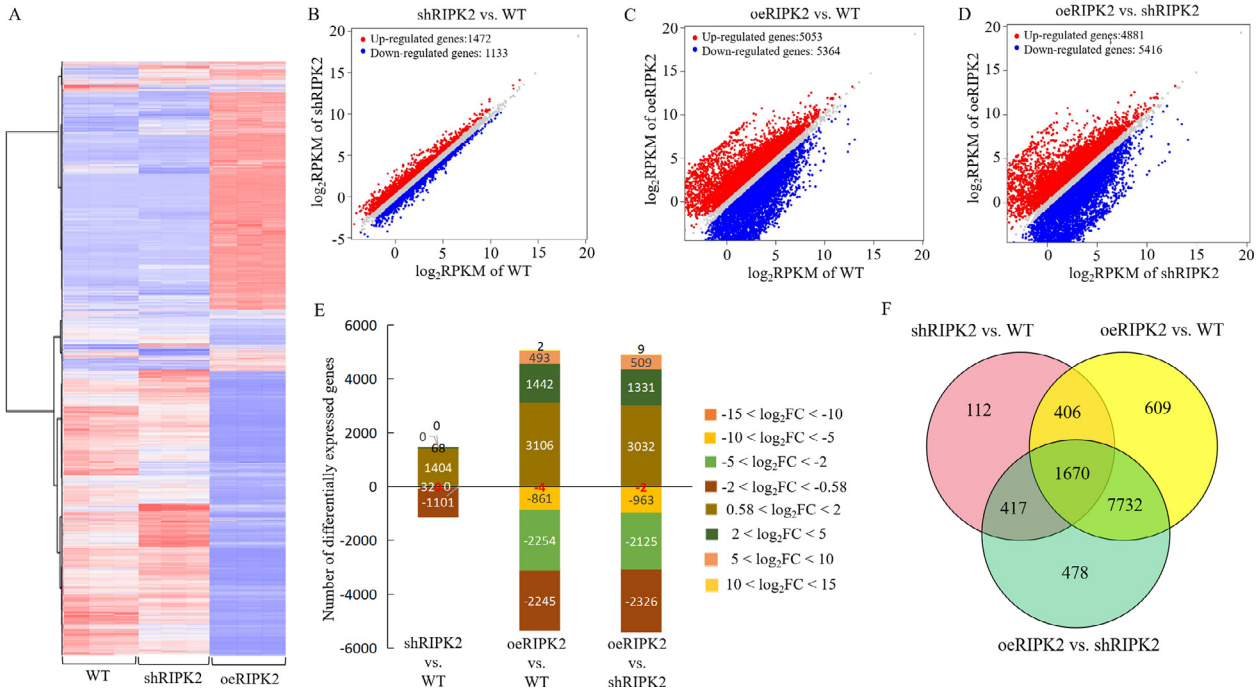

Figure 6. RNA-seq profling in the comparisons of *RIPK2* knockdown HD11 cells (shRIPK2) vs. wild type HD11 cells (WT), *RIPK2* overexpression HD11 cells (oeRIPK2) vs. WT, and oeRIPK2 vs. shRIPK2. (A) Heatmap analysis for the transcriptome data from the WT, shRIPK2, and oeRIPK2 group. Red color indicates upregulation, while blue color means downregulation. (B–D) The expression levels of differentially expressed genes (DEGs) in the comparison of shRIPK2 vs. WT (B), oeRIPK2 vs. WT (C), and oeRIPK2 vs. shRIPK2 (D). Red spots represent DEGs for upregulation, blue spots for downregulation, and grey spots for unchanged genes in the comparisons. E. The distribution of $\log_2$(fold changes) of differentially expressed genes (DEGs) in the comparisons of shRIPK2 vs. WT, oeRIPK2 vs. WT, and oeRIPK2 vs. shRIPK2. F. Overlap in differentially expressed genes (DEGs) for the comparisons of shRIPK2 vs. WT, oeRIPK2 vs. WT, and oeRIPK2 vs. shRIPK2.

for relative expression analysis by RT-qPCR (Figure 8). The results showed that the relative expression of *JUN, FOS, BCL2L11, CD44, CD36, TNFSF8, PDK4, IRF1*, and *CXCR1* in oeRIPK2 group were significantly lower than those in WT and shRIPK2 group ($P < 0.01$), whereas the relative expression of *HSPB1, CASP3*, and *PAK3* in oeRIPK2 group were significantly higher than those in WT and shRIPK2 group. The expression tendency (upregulated or downregulated) of the aforementioned DEGs in the comparison of shRIPK2 vs. WT was completely opposite to those in oeRIPK2 vs. WT and oeRIPK2 vs. shRIPK2. The results of RT-qPCR validation were consistent with RNA-seq data, which confirms the reliability of the RNA-seq results.

RIPK2 *is a Critical Regulator for TGF-Beta Signaling Pathway*

In the current study, TGF-beta signaling pathway was significantly activated with *RIPK2* overexpression or silenced. A total of 34 and 28 upregulated DEGs were involved in TGF-beta signaling pathway in oeRIPK2 vs. WT and oeRIPK2 vs. shRIPK2, respectively, as shown in Tables S6 and S7. 46 DEGs were commonly involved in the TGF-beta signaling pathway in both oeRIPK2 vs. WT and oeRIPK2 vs shRIPK2 (Figure 9A). The fold change of the overlapped DEGs ranged from −49.15 to 89.23 and from −39.44 to 82.18 in the comparison of oeRIPK2 vs. WT and oeRIPK2 vs. shRIPK2, respectively (Tables S6 and 7). To further corroborate the correlation between *RIPK2* and TGF-beta signaling pathway, we used RT-qPCR and western blotting to identify the expression level of TGFB1 and TGFB3 with the *RIPK2* gene overexpression or silenced. As shown in Figures 9B–9F, the mRNA and protein levels of TGFB1 or TGFB3 showed remarkable increase in the comparison of oeRIPK2 vs. WT, which is in agreement with the RNA-seq data. However, compared to the WT group, the mRNA and protein expression level of TGFB1 or TGFB3 were significantly decreased in the shRIPK2 group (Figures 9B–9F). These results indicate *RIPK2* is involved in the regulation of *TGFB1* and *TGFB3* in a certain relationship to further modulate the TGF-beta signaling pathway.

DISCUSSION

Receptor interacting protein kinase (**RIPK**) family has 5 important members in chicken, including RIPK1, 2, 3, 4, and 5. However, there were 8 members (RIPK1, 2, 3, 4, 5, 6, 7, and 8) of RIPK in human. Currently, among the members of RIPK family, researchers mainly focused on the *RIPK2* gene, since it is the key and core gene in NOD signaling pathway. *RIPK2* plays an important role in protecting the body from a variety of stimuli and pathological conditions (Zhao et al., 2017; Pham et al., 2020; Honjo et al., 2021). Although there have been many studies on *RIPK2* in humans and mice,

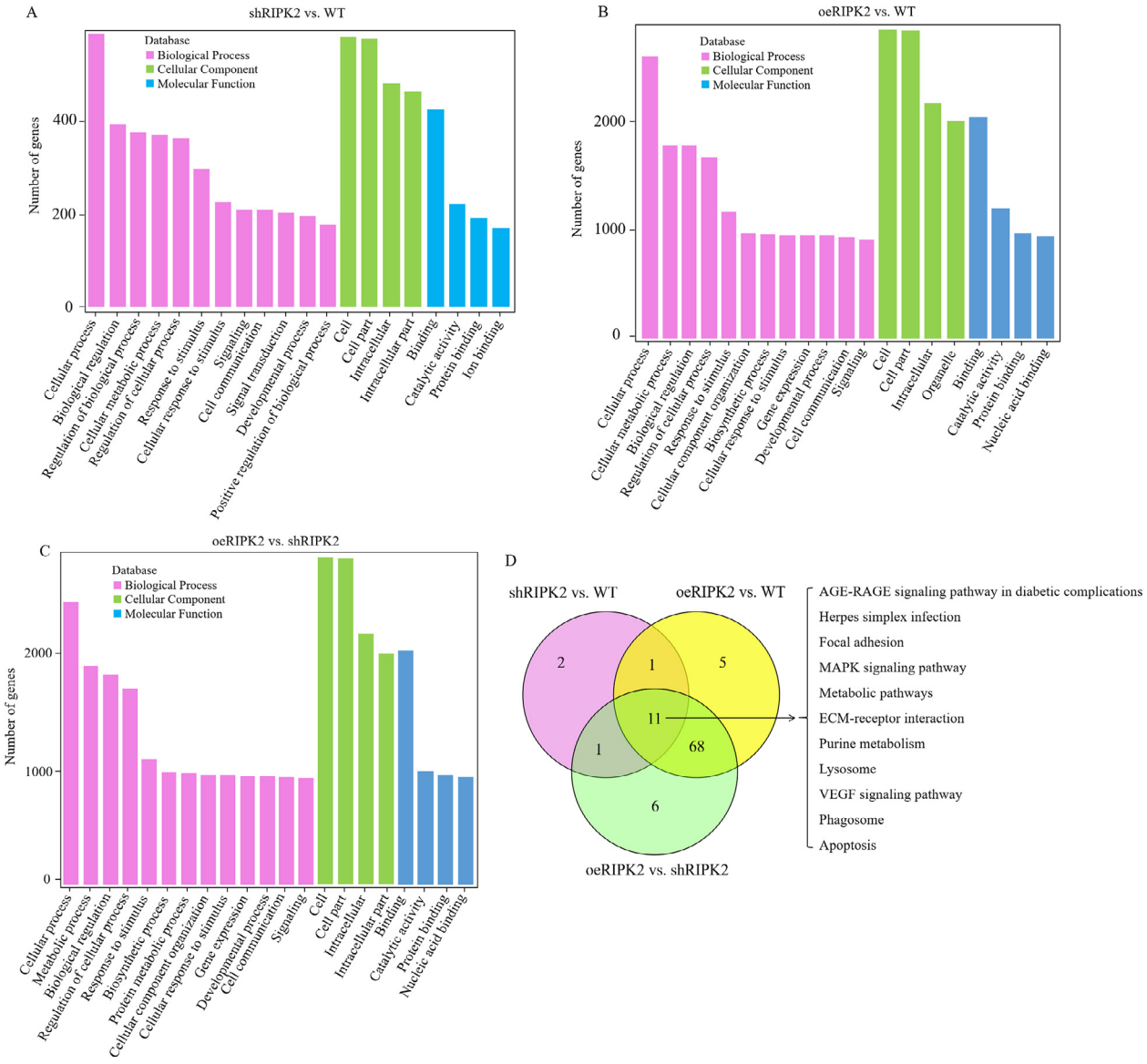

Figure 7. Gene classification was based on Gene Ontology (GO) and Kyoto Encyclopedia of Genes and Genomes (KEGG) analysis for differentially expressed genes (DEGs). (A–C) Different classes are shown for biological processes, cellular components, and molecular functions in the comparisons of *RIPK2* knockdown HD11 cells (shRIPK2) vs. wild type HD11 cells (WT) (A), RIPK2 overexpression HD11 cells vs. WT (B), and oeRIPK2 vs. shRIPK2 (C). (D) Overlap in significantly changed pathways for the comparisons of shRIPK2 vs. WT, oeRIPK2 vs. WT, and oeRIPK2 vs. shRIPK2.

its regulatory gene network in poultry has not been carried out. This study is the first to demonstrate the essential genes or pathways, as well as the downstream targets regulated by *RIPK2* through transcriptome analysis.

Chicken *RIPK2* is located on chromosome 2 and contains 12 exons. In the current study, the expression level of *RIPK2* gene in 13 tissues was analyzed. It was found that chicken bone marrow had the highest *RIPK2* expression level, which is consistent with the previous findings in human (Fagerberg et al., 2014). However, the expression level of *RIPK2* in liver was different between human and chicken (Fagerberg et al., 2014). Herein, we found that inhibition of chicken *RIPK2* can attenuate the LPS-induced cell injuries, which is consistent with the findings in human and mice. To further identify the gene networks or pathways regulated by *RIPK2*, we compared the transcriptomes of each 2 groups (WT, shRIPK2, and oeRIPK2) to find the significantly changed genes and pathways. It was found that Focal adhesion, MAPK signaling pathway, ECM-receptor interaction, Lysosome, VEGF signaling pathway, Phagosome, and Apoptosis were commonly significantly changed in the three comparisons (shRIPK2 vs. WT, oeRIPK2 vs. WT, and oeRIPK2 vs. shRIPK2). Yang et al. demonstrated that knockdown of *RIPK2* could inhibit the apoptosis pathway in human gastric cancer (Yang et al., 2021). Moreover, Pan et al. and Cai et al. have separately reported that silencing of *RIPK2* suppressed the MAPK signaling pathway (Cai et al., 2018; Pan et al., 2021). The aforementioned research findings were in agreement with current results. Furthermore, we found Focal adhesion, ECM-receptor interaction, Lysosome, VEGF signaling pathway, and Phagosome were

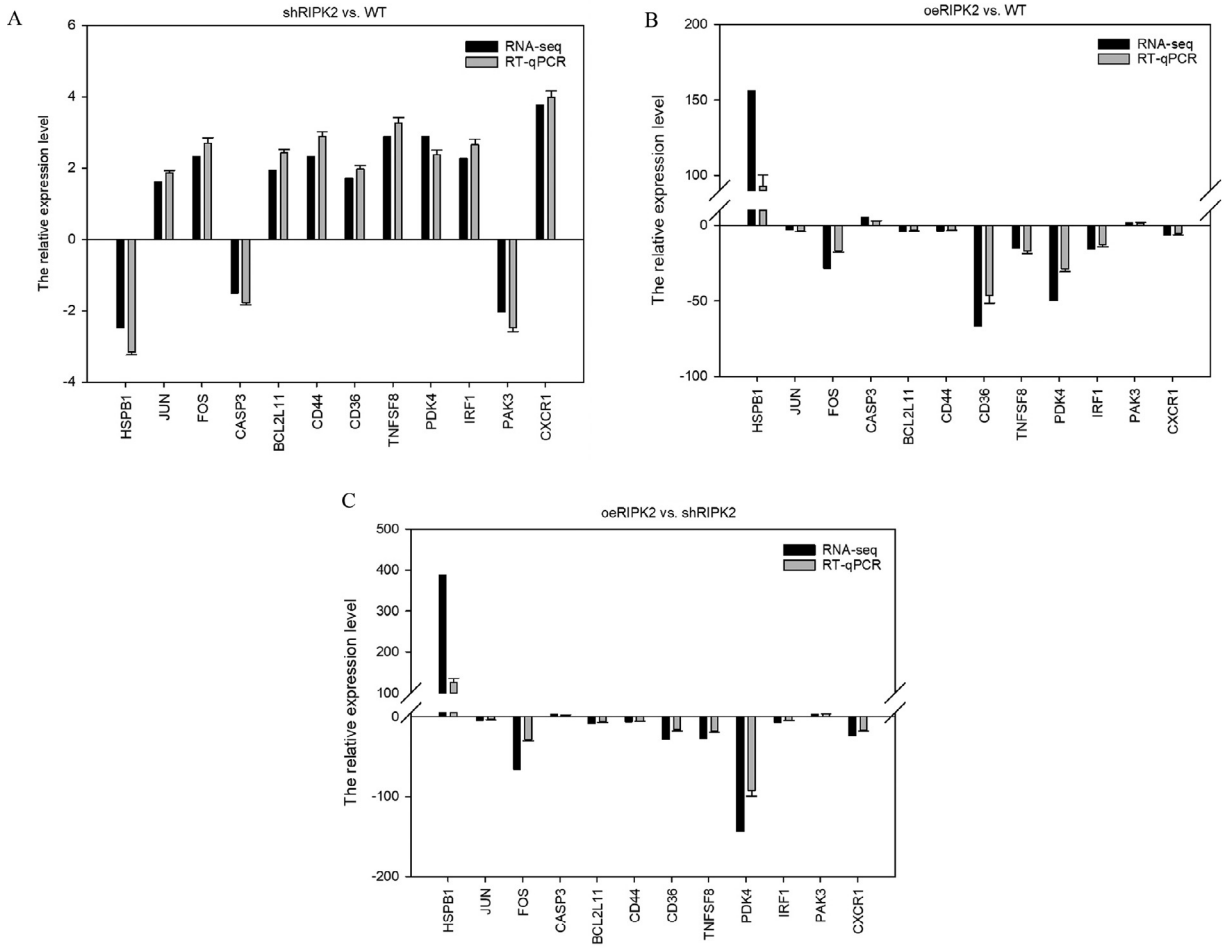

Figure 8. Evaluation and comparison of mRNA expression levels of the selected differentially expressed genes (DEGs) by using RNA-seq and RT-qPCR for different comparisons. (A−C) The mRNA expression level of the differentially expressed genes in the comparisons of *RIPK2* knockdown HD11 cells (shRIPK2) vs. wild type HD11 cells (WT) (A), *RIPK2* overexpression HD11 cells (oeRIPK2) vs. WT (B), and oeRIPK2 vs. shRIPK2 (C).

closely correlated with *RIPK2* regulation. These results were reasonable and expected, since *RIPK2* was involved in cellular immune response (Usluoglu et al., 2007; Sandford et al., 2011; Sun et al., 2015, 2016) and knockdown of *RIPK2* could avoid the excessive tissues/cells injury and inflammatory response (Wu et al., 2012; Rahman et al., 2014; Yang et al., 2021).

Moreover, it was worth to note that the TGF-beta signaling pathway was also detected to be significantly changed in the comparison of oeRIPK2 vs. WT and oeRIPK2 vs. shRIPK2. The TGF-beta signaling pathway plays an important role in the development, homeostasis, and repair of most tissues in organisms (Kitisin et al., 2007; Chen et al., 2012; Tzavlaki and Moustakas, 2020). It has been demonstrated that TGF-beta signaling pathway presents broad therapeutic potential in many diseases, including various cancers, hepatic fibrosis, inflammatory bowel disease etc. (Xu et al., 2016; Colak and Ten Dijke, 2017; Ihara et al., 2017). Since *TGFB1* and *TGFB3* were the initiation genes of chicken TGF-beta signaling pathway, we subsequently validated the relationship between *RIPK2* and *TGFB1*/*TGFB3*. Our transcriptome data showed that *TGFB1* and *TGFB3* were significantly increased in the comparisons of oeRIPK2 vs. WT (Fold change of *TGFB1* = 3.14; Fold change of *TGFB3* = 8.04) and oeRIPK2 vs. shRIPK2 (Fold change of *TGFB1* = 2.45; Fold change of *TGFB3* = 10.75). Moreover, we validated these results finding decreased expression levels of both mRNA and protein for TGFB1 and TGFB3 in shRIPK2 group, compared to WT. However, data obtained by RT-qPCR and western blot showed the expression of TGFB1 and TGFB3 were significantly upregulated in the comparison of oeRIPK2 vs. shRIPK2. These results strongly suggested *TGFB1* and *TGFB3* were the downstream targets of *RIPK2* and positively modulated by *RIPK2* in chicken HD11 cells.

It has been demonstrated that the *TGFB1* has the function to regulate cell proliferation, differentiation and growth, and can modulate expression and activation of other growth factors including interferon gamma and tumor necrosis factor alpha (Lafontaine et al., 2011; Ma et al., 2019; Moraveji et al., 2019). *TGFB3* is involved in embryogenesis and cell differentiation, and may play a role in wound healing (Lichtman et al., 2016; Stockis et al., 2017; Tamayo et al., 2018). It has been

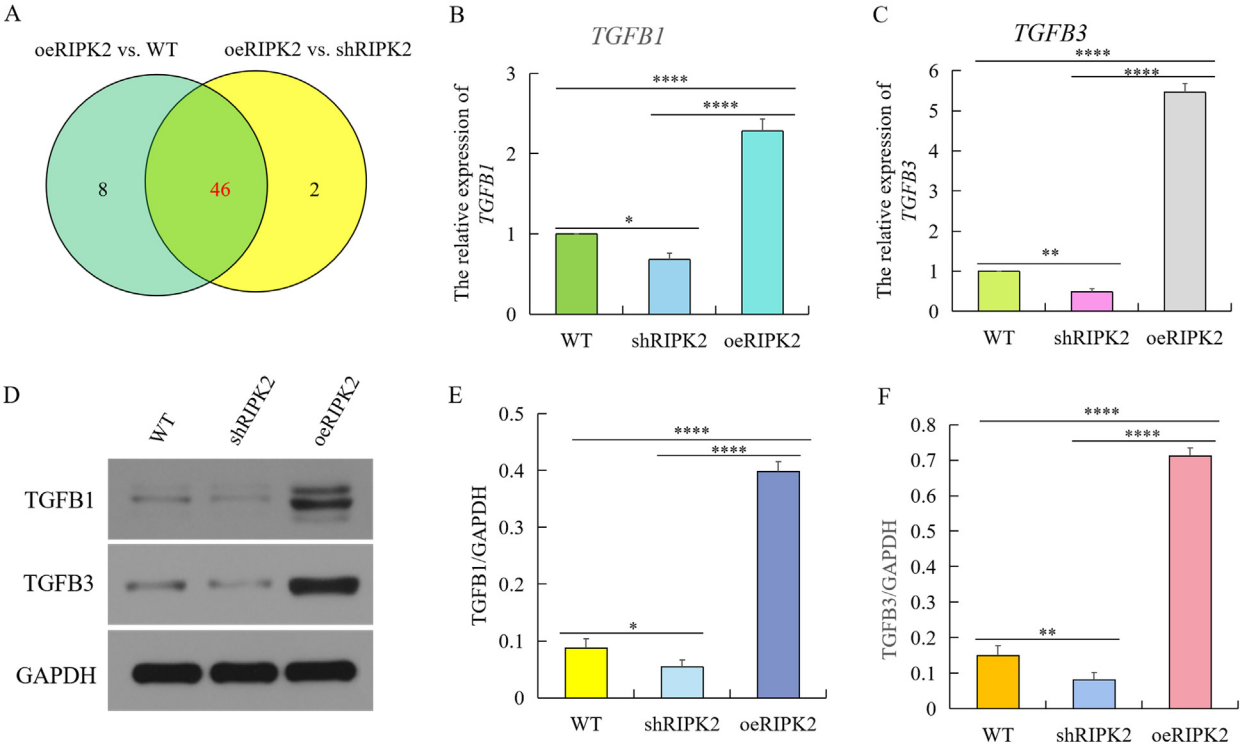

Figure 9. New target genes of chicken *RIPK2*. (A) Overlap differentially expressed genes of TGF-beta signaling pathway in the comparisons of *RIPK2* overexpression HD11 cells (oeRIPK2) vs. wild type HD11 cells (WT) and oeRIPK2 vs. *RIPK2* knockdown HD11 cells (shRIPK2). (B and C) The relative *TGFB1* (B) and *TGFB3* (C) mRNA expression level in the group of wild type HD11 cells (WT), knockdown of *RIPK2* HD11 cells (shRIPK2), and overexpression of *RIPK2* HD11 cells (oeRIPK2). (D) The protein level of TGFB1 and TGFB3 in the group of wild type HD11 cells (WT), knockdown of RIPK2 HD11 cells (shRIPK2), and overexpression of RIPK2 HD11 cells (oeRIPK2). * $P < 0.05$; ** $P < 0.01$; **** $P < 0.0001$. All values are mean±SD. n = 4.

reported that mutation of *TGFB3* is a cause of aortic aneurysms and dissections, as well as familial arrhythmogenic right ventricular dysplasia 1 (Beffagna et al., 2005; Bertoli-Avella et al., 2015). According to our results, *RIPK2* has the potential ability to involve in cell proliferation, differentiation, growth, and different disease via regulating the TGF-beta signaling pathway.

CONCLUSIONS

In summary, this study has provided an analysis of the genetic landscape associated with *RIPK2* knockdown or overexpresion in chicken HD11 macrophages. In total, 2,605, 10,469, and 10,297 DEGs were identified in shRIPK2 vs. WT, oeRIPK2 vs. WT, and oeRIPK2 vs. shRIPK2, respectively. Functional annotation analysis showed that apoptosis, MAPK, p53, ECM-receptor interaction, Lysosome, VEGF signaling pathway, Phagosome, and TGF-beta signaling pathway were involved in *RIPK2* knockdown/overexpression HD11 cells. By analyzing the enriched pathway and gene networks, we identified that TGF-beta signaling pathway, especially the initiation genes *TGFB1* and *TGFB3*, were targeted by *RIPK2* gene. As a whole, this study can not only provide data support for constructing gene networks related to *RIPK2*, but also provide new ideas for the functions of *RIPK2*.

ACKNOWLEDGMENTS

This research was supported by the National Natural Science Foundation of China (Grant No. 31802053), The Natural Science Foundation of Jiangsu Province (Grant No. BK20180907), the China Postdoctoral Science Foundation (2019M661950), Jiangsu Postdoctoral Science Foundation (137070510), Jiangsu Graduate Research and Practice Innovation Program, grant number SJCX22_1796, and Science and Technology Innovation Fund of Yangzhou University (X20220654),

DISCLOSURES

The authors declare that they have no conflict of interest.

SUPPLEMENTARY MATERIALS

Supplementary material associated with this article can be found in the online version at doi:10.1016/j.psj.2022.102263.

REFERENCES

Anand, P. K., S. W. G. Tait, M. Lamkanfi, A. O. Amer, G. Nunez, G. Pagès, J. Pouysségur, M. A. McGargill, D. R. Green, and T. D. Kanneganti. 2011. TLR2 and RIP2 pathways mediate autophagy of Listeria monocytogenes via extracellular signal-

regulated kinase (ERK) activation. J. Biol. Chem. 286:42981–42991.
Balamayooran, T., S. Batra, G. Balamayooran, S. Cai, K. S. Kobayashi, R. A. Flavell, and S. Jeyaseelan. 2011. Receptor-interacting protein 2 controls pulmonary host defense to Escherichia coli infection via the regulation of interleukin-17A. Infect. Immun. 79:4588–4599.
Beffagna, G., G. Occhi, A. Nava, L. Vitiello, A. Ditadi, C. Basso, B. Bauce, G. Carraro, G. Thiene, J. A. Towbin, G. A. Danieli, and A. Rampazzo. 2005. Regulatory mutations in transforming growth factor-β3 gene cause arrhythmogenic right ventricular cardiomyopathy type 1. Cardiovasc. Res. 65:366–373.
Bertoli-Avella, A. M., E. Gillis, H. Morisaki, J. M. A. Verhagen, B. M. De Graaf, G. Van De Beek, E. Gallo, B. P. T. Kruithof, H. Venselaar, L. A. Myers, S. Laga, A. J. Doyle, G. Oswald, G. W. A. Van Cappellen, I. Yamanaka, R. M. Van Der Helm, B. Beverloo, A. De Klein, L. Pardo, M. Lammens, C. Evers, K. Devriendt, M. Dumoulein, J. Timmermans, H. T. Bruggenwirth, F. Verheijen, I. Rodrigus, G. Baynam, M. Kempers, J. Saenen, E. M. Van Craenenbroeck, K. Minatoya, R. Matsukawa, T. Tsukube, N. Kubo, R. Hofstra, M. J. Goumans, J. A. Bekkers, J. W. Roos-Hesselink, I. M. B. H. Van De Laar, H. C. Dietz, L. Van Laer, T. Morisaki, M. W. Wessels, and B. L. Loeys. 2015. Mutations in a TGF-β ligand, TGFB3, cause syndromic aortic aneurysms and dissections. J. Am. Coll. Cardiol. 65:1324–1336.
Bist, P., N. Dikshit, T. H. Koh, A. Mortellaro, T. T. Tan, and B. Sukumaran. 2014. The Nod1, Nod2, and Rip2 axis contributes to host immune defense against intracellular Acinetobacter baumannii infection. Infect. Immun. 82:1112–1122.
Cai, X., Y. Yang, W. Xia, H. Kong, M. Wang, W. Fu, Minh. I. Long, Y. H. A. Hu, and D. Xu. 2018. RIP2 promotes glioma cell growth by regulating TRAF3 and activating the NF-κB and p38 signaling pathways. Oncol. Rep. 39:2915–2923.
Chen, G., C. Deng, and Y. P. Li. 2012. TGF-β and BMP signaling in osteoblast differentiation and bone formation. Int. J. Biol. Sci. 8:272–288.
Colak, S., and P. Ten Dijke. 2017. Targeting TGF-beta signaling in cancer. Trends in Cancer 3:56–71.
Fagerberg, L., B. M. Hallstrom, P. Oksvold, C. Kampf, D. Djureinovic, J. Odeberg, M. Habuka, S. Tahmasebpoor, A. Danielsson, K. Edlund, A. Asplund, E. Sjostedt, E. Lundberg, C. A. K. Szigyarto, M. Skogs, J. Ottosson Takanen, H. Berling, H. Tegel, J. Mulder, P. Nilsson, J. M. Schwenk, C. Lindskog, F. Danielsson, A. Mardinoglu, A. Sivertsson, K. Von Feilitzen, M. Forsberg, M. Zwahlen, I. Olsson, S. Navani, M. Huss, J. Nielsen, F. Ponten, and M. Uhlen. 2014. Analysis of the human tissue-specific expression by genome-wide integration of transcriptomics and antibody-based proteomics. Mol. Cell. Proteomics 13:397–406.
Hofmann, S. R., L. Girschick, R. Stein, and F. Schulze. 2021. Immune modulating effects of receptor interacting protein 2 (RIP2) in autoinflammation and immunity. Clin. Immunol. 223:108648.
Honjo, H., T. Watanabe, K. Kamata, K. Minaga, and M. Kudo. 2021. RIPK2 as a new therapeutic target in inflammatory bowel diseases. Front. Pharmacol. 12:1–9.
Huang, D. W., B. T. Sherman, and R. A. Lempicki. 2009a. Bioinformatics enrichment tools: paths toward the comprehensive functional analysis of large gene lists. Nucleic Acids Res. 37:1–13.
Huang, D. W., B. T. Sherman, and R. A. Lempicki. 2009b. Systematic and integrative analysis of large gene lists using DAVID bioinformatics resources. Nat. Protoc. 4:44–57.
Ihara, S., Y. Hirata, and K. Koike. 2017. TGF-β in inflammatory bowel disease: a key regulator of immune cells, epithelium, and the intestinal microbiota. J. Gastroenterol. 52:777–787.
Jing, H., L. Fang, D. Wang, Z. Ding, R. Luo, H. Chen, and S. Xiao. 2014. Porcine reproductive and respiratory syndrome virus infection activates NOD2-RIP2 signal pathway in MARC-145 cells. Virology 458−459:162–171.
Kanehisa, M., and S. Goto. 2000. KEGG: Kyoto Encyclopedia of Genes and Genomes. Nucleic Acids Res 28:27–30.
Kitisin, K., T. Saha, T. Blake, N. Golestaneh, M. Deng, C. Kim, Y. Tang, K. Shetty, B. Mishra, and L. Mishra. 2007. Tgf-Beta signaling in development. Sci. STKE 2007:1–5.
Lafontaine, L., P. Chaudhry, M. J. Lafleur, C. Van Themsche, M. J. Soares, and E. Asselin. 2011. Transforming growth factor beta regulates proliferation and invasion of rat placental cell lines. Biol. Reprod. 84:553–559.
Li, S., P. Deng, M. Wang, X. Liu, M. Jiang, B. Jiang, L. Yang, and J. Hu. 2019. IL-1α and IL-1β promote NOD2-induced immune responses by enhancing MAPK signaling. Lab. Investig. 99:1321–1334.
Lichtman, M. K., M. Otero-Vinas, and V. Falanga. 2016. Transforming growth factor beta (TGF-β) isoforms in wound healing and fibrosis. Wound Repair Regen 24:215–222.
Lin, H. Bin, K. Naito, Y. Oh, G. Farber, G. Kanaan, A. Valaperti, F. Dawood, L. Zhang, G. H. Li, D. Smyth, M. Moon, Y. Liu, W. Liang, B. Rotstein, D. J. Philpott, K. H. Kim, M. E. Harper, and P. P. Liu. 2020. Innate immune Nod1/RIP2 signaling is essential for cardiac hypertrophy but requires mitochondrial antiviral signaling protein for signal transductions and energy balance. Circulation 142:2240–2258.
Ma, L., Z. Q. Yang, J. L. Ding, S. Liu, B. Guo, and Z. P. Yue. 2019. Function and regulation of transforming growth factor β1 signalling in antler chondrocyte proliferation and differentiation. Cell Prolif 52:e12637.
Miller, M. H., M. G. Shehat, and J. T. Tigno-Aranjuez. 2020. Immune modulation of allergic asthma by early pharmacological inhibition of RIP2. ImmunoHorizons 4:825–836.
Moraveji, S. F., F. Esfandiari, S. Taleahmad, S. Nikeghbalian, F. A. Sayahpour, N. S. Masoudi, A. Shahverdi, and H. Baharvand. 2019. Suppression of transforming growth factor-beta signaling enhances spermatogonial proliferation and spermatogenesis recovery following chemotherapy. Hum. Reprod. 34:2430–2442.
Pan, D. S., Y. Lyu, N. Zhang, X. Wang, T. Lei, and Z. Liang. 2021. RIP2 knockdown inhibits cartilage degradation and oxidative stress in IL-1β-treated chondrocytes via regulating TRAF3 and inhibiting p38 MAPK pathway. Clin. Immunol. 232:108868.
Peighambari, S. M., R. J. Julian, and C. L. Gyles. 2000. Experimental Escherichia coli respiratory infection in broilers. Avian Dis. 44:759.
Pham, O. H., B. Lee, J. Labuda, A. M. Keestra-Gounder, M. X. Byndloss, R. M. Tsolis, and S. J. McSorley. 2020. NOD1/NOD2 and rip2 regulate endoplasmic reticulum stress-induced inflammation during chlamydia infection. MBio 11:e00979-20.
Rahman, M. A., K. Sundaram, S. Mitra, M. A. Gavrilin, and M. D. Wewers. 2014. Receptor interacting protein-2 plays a critical role in human lung epithelial cells survival in response to Fas-induced cell-death. PLoS One 9:e92731.
Sandford, E. E., M. Orr, E. Balfanz, N. Bowerman, X. Li, H. Zhou, T. J. Johnson, S. Kariyawasam, P. Liu, L. K. Nolan, and S. J. Lamont. 2011. Spleen transcriptome response to infection with avian pathogenic Escherichia coli in broiler chickens. BMC Genomics 12:1–13.
Shaw, P. J., M. J. Barr, J. R. Lukens, M. A. McGargill, H. Chi, T. W. Mak, and T. D. Kanneganti. 2011. Signaling via the RIP2 adaptor protein in central nervous system-infiltrating dendritic cells promotes inflammation and autoimmunity. Immunity 34:75–84.
Shimada, K., S. Chen, P. W. Dempsey, R. Sorrentino, R. Alsabeh, A. V. Slepenkin, E. Peterson, T. M. Doherty, D. Underhill, T. R. Crother, and M. Arditi. 2009. The NOD/RIP2 pathway is essential for host defenses against Chlamydophila pneumoniae lung infection. PLoS Pathog. 5:e1000379.
Stockis, J., O. Dedobbeleer, and S. Lucas. 2017. Role of GARP in the activation of latent TGF-β1. Mol. Biosyst. 13:1925–1935.
Sun, H., P. Liu, L. K. Nolan, and S. J. Lamont. 2015. Avian pathogenic Escherichia coli (APEC) infection alters bone marrow transcriptome in chickens. BMC Genomics 16:1–15.
Sun, H., P. Liu, L. K. Nolan, and S. J. Lamont. 2016. Thymus transcriptome reveals novel pathways in response to avian pathogenic Escherichia coli infection. Poult. Sci. 95:2803–2814.
Tamayo, E., P. Alvarez, and R. Merino. 2018. TGFβ superfamily members as regulators of B cell development and function—implications for autoimmunity. Int. J. Mol. Sci. 19:3928.
Tzavlaki, K., and A. Moustakas. 2020. TGF-β signaling. Biomolecules 10:1–38.
Usluoglu, N., J. Pavlovic, K. Moelling, and G. Radziwill. 2007. RIP2 mediates LPS-induced p38 and IκBα signaling including IL-12 p40

expression in human monocyte-derived dendritic cells. Eur. J. Immunol. 37:2317–2325.

Wu, X. M., W. Q. Chen, Y. W. Hu, L. Cao, P. Nie, and M. X. Chang. 2018. RIP2 is a critical regulator for NLRs signaling and MHC antigen presentation but not for MAPK and PI3K/Akt pathways. Front. Immunol. 9:726.

Wu, S., T. Kanda, S. Nakamoto, F. Imazeki, and O. Yokosuka. 2012. Knockdown of receptor-interacting serine/threonine protein kinase-2 (RIPK2) affects EMT-associated gene expression in human hepatoma cells. Anticancer Res 32:3775–3784.

Xu, F., C. Liu, D. Zhou, and L. Zhang. 2016. TGF-β/SMAD pathway and its regulation in hepatic fibrosis. J. Histochem. Cytochem. 64:157–167.

Yang, Q., S. Tian, Z. Liu, and W. Dong. 2021. Knockdown of RIPK2 inhibits proliferation and migration, and induces apoptosis via the NF-κB signaling pathway in gastric cancer. Front. Genet. 12:1–13.

Zhao, C. H., X. Ma, H. Y. Guo, P. Li, and H. Y. Liu. 2017. RIP2 deficiency attenuates cardiac hypertrophy, inflammation and fibrosis in pressure overload induced mice. Biochem. Biophys. Res. Commun. 493:1151–1158.

Zhou, Y., L. Hu, W. Tang, D. Li, L. Ma, H. Liu, S. Zhang, X. Zhang, L. Dong, X. Shen, S. Chen, R. Xue, and S. Zhang. 2021. Hepatic NOD2 promotes hepatocarcinogenesis via a RIP2-mediated proinflammatory response and a novel nuclear autophagy-mediated DNA damage mechanism. J. Hematol. Oncol. 14:1–19.